Two-particle self-consistent approach for broken symmetry phases

Lorenzo Del Re,

Max-Planck-Institute for Solid State Research, 70569 Stuttgart, Germany
l.delre@fkf.mpg.de

July 1, 2024

Abstract

Spontaneous symmetry breaking of interacting fermion systems constitutes a major challenge for many-body theory due to the proliferation of new independent scattering channels once absent or degenerate in the symmetric phase. One example is given by the ferro/antiferromagnetic broken symmetry phase (BSP) of the Hubbard model, where vertices in the spin-transverse and spin-longitudinal channels become independent with a consequent increase in the computational power for their calculation. Here we generalize the formalism of the non-perturbative Two-Particle-Self-Consistent method (TPSC) to treat broken SU(2) magnetic phases of the Hubbard model, providing with a efficient yet reliable method. We show that in the BSP, the sum-rule enforcement of susceptibilities must be accompanied by a modified gap equation resulting in a renormalisation of the order parameter, vertex corrections and the preservation of the gap-less feature of the Goldstone modes. We then apply the theory to the antiferromagnetic phase of the Hubbard model in the cubic lattice at half-filling. We compare our results of double occupancies and staggered magnetisation to the ones obtained using Diagrammatic Monte Carlo showing excellent quantitative agreement. We demonstrate how vertex corrections play a central role in lowering the Higgs resonance with respect to the quasi-particle excitation gap in the spin-longitudinal susceptibility, yielding a well visible Higgs-mode.

Contents

1 Introduction

The characterization of broken symmetry phases (BSP) in correlated quantum systems remains a formidable challenge for many-body theory. In fact, determining the precise ground state of spin Hamiltonians, such as the 3D-Heisenberg model with antiferromagnetic exchange, remains an open question to this day. Even if the precise knowledge of the groundstate might remain out of reach, it is possible to improve mean-field predicted groundstates , e.g. the Néel state, including quantum corrections encoded in the long-range and low-energy Goldstone modes [1, 2, 3, 4, 5], e.g. spin-waves in antiferromagnets [6].

The situation becomes richer when interacting electrons in solids get strongly correlated. A minimal model to describe correlated materials is given by the Hubbard model [7], where electrons interact via on-site Coulomb repulsion that enhances electron localisation [8]. The theoretical challenge with strongly correlated BSP consists in taking into account at the same time the long-range fluctuations encoded in the Goldstone modes and localisation of electrons.

Such an ambitious task could be achieved by employing cluster [9] or diagrammatic [10] extensions of Dynamical Mean Field Theory (DMFT) [11], or Diagrammatic Monte Carlo (DiagMC) [12, 13]. However, the inclusion of long-range modes for cluster theories would be limited by the maximum size of the cluster used in the calculations. In diagrammatic approaches, the proliferation of independent vertex components [14, 15, 16, 17, 18, 19, 20], once absent or degenerate in the symmetric phase, strongly increases the computational power needed for their numerical evaluation.

Hence, it is of great interest to develop efficient algorithms requiring less computational resources but that at the same time are able to include correlation effects. In this realm, the Two-Particle-Self-Consistent (TPSC) approach [21, 22, 23, 24, 25, 26, 27, 28] has been proven to be a reliable and efficient method to describe the physics of the Hubbard model in the weak-to-intermediate interaction regime. Given its reduced computational complexity, TPSC has already been successfully extended to multi-orbital models [25], interfaced with *ab-intio* calculations [26] and applied to non-equilibrium [27]. However, TPSC formulations available today can only treat symmetric phases, which prevents the application of the theory to parameter regimes where materials are found in BSP. Furthermore, since TPSC uses Moriya corrections to two-particle propagators masses [29, 30, 31, 32, 33] for including correlation effects, a straightforward generalisation of TPSC equations could violate Goldstone's theorem introducing an unphysical energy gap to the Goldstone modes. In this work, we show how to properly extend the TPSC formalism to the case of spontaneous symmetry breaking, which correctly preserves the Goldstone modes. We apply the new formulation to the antiferromagnetic phase of the three-dimensional Hubbard model in the cubic lattice. We compared our results with DiagMC [13] showing an excellent quantitative agreement for a wide range of interaction values. We show that the degree of correlation is reduced by decreasing temperature from the critical value, extending the range of applicability of the theory to higher values of the interactions deep in the BSP. We demonstrate how symmetry breaking implies a differentiation of vertex corrections in different scattering channels, which play a central role in lowering the Higgs resonance with respect to the quasi-particle excitation gap in the spin-longitudinal susceptibility, yielding a well visible Higgs-mode. The stage is yours. Write your article here. The bulk of the paper should be clearly divided into sections with short descriptive titles, including an introduction and a conclusion.

2 The model

In this work we will explicitly consider the single band Hubbard model in the cubic lattice,

$$H = -t \sum_{\langle ij \rangle \sigma} c^{\dagger}_{i\sigma} c_{j\sigma} + U \sum_{i} \hat{n}_{i\uparrow} \hat{n}_{i\downarrow}, \tag{1}$$

where t is the electronic hopping amplitude between nearest-neighbors and U is the local Coulomb repulsion. In the case of the AF phase, the system loses the full translational symmetry of the original cubic lattice and it is useful to introduce the sub-lattice index $a = A, B$ for specifying whether the fermionic field $c^{\dagger}_{ia\sigma}$ is evaluated at one site belonging to the sub-lattice A or B.

3 The method

3.1 The TPSC ansatz

The starting point of TPSC consists in assuming an approximate form of the electron self-energy. In particular, we assume the following ansatz for the self-energy:

$$\Sigma^{ab}_{\sigma\sigma'}(x, y) = \delta(x - y) \delta_{ab} \, \lambda \, U \left(\delta_{\sigma\sigma'} n_{a\bar{\sigma}} - \delta_{\sigma\bar{\sigma}'} s^{\sigma\bar{\sigma}}_{a} \right), \tag{2}$$

where $x = (\mathbf{R}, \tau)$ is a quadrivector containing the lattice coordinates ($\mathbf{R}$) and the imaginary time (τ), $n_{a\sigma} = \left\langle c^{\dagger}_{ia\sigma} c_{ia\sigma} \right\rangle$, $s^{\sigma\sigma'}_{a} = \left\langle c^{\dagger}_{ia\sigma'} c_{ia\sigma} \right\rangle$, and:

$$\lambda = \frac{\langle \hat{n}_{\uparrow} \hat{n}_{\downarrow} \rangle}{n_{\uparrow} n_{\downarrow}}, \tag{3}$$

which is the same prefactor appearing in the paramagnetic case [22, 24, 34]. In the next section, we will see how the parameter λ, or equivalently the double occupancies, can be evaluated self-consistently together with the order parameter, by imposing specific sum rules of physical susceptibilities.

We notice that in the AF phase the off-diagonal components of the self-energy in the spin indices should vanish, i.e. $s^{\sigma\bar{\sigma}} = 0$. However, it is useful to keep those terms in the expression of the self-energy for the derivation of the Bethe-Salpeter equation in the spin-transverse channel. Therefore, we will consider the presence of an external field that breaks spin-conservation to compute the functional derivatives of Σ with respect to the off-diagonal component of the propagator evaluated in the limit of a vanishing field.

In Appendix A we show that the expression for Σ in Eq.(2) can be derived starting from the equation of motion and by performing an approximation at the two-particle level that preserves an exact constraint in the limit of equal times and positions.

In order to obtain self-consistency at the two-particle level, we have to calculate physical susceptibilities and therefore we need the knowledge of the irreducible vertex function Γ, which is obtained by carrying the functional derivative of Σ with respect to G, i.e. $\Gamma(1,2,3,4) = \frac{\delta\Sigma(2,1)}{\delta G(3,4)}$ [35].

In the FM/AF phases the original SU(2) symmetry of the Hubbard Hamiltonian is spontaneously broken and the two independent scattering channels to be considered are the spin-transverse and spin-longitudinal channels [17].

3.1.1 Spin-transverse channel

The vertex function in the spin-transverse channel is defined as:

$$\begin{aligned}\Gamma^{abcd}_{\overline{\uparrow\downarrow}}(x_1,x_2,x_3,x_4) &= \frac{\delta\Sigma^{ba}_{\downarrow\uparrow}(x_2,x_1)}{\delta G^{cd}_{\downarrow\uparrow}(x_3,x_4)} \\ &= -\lambda U \delta_{ab}\delta_{ac}\delta_{ad}\delta(x_1-x_2)\delta(x_1-x_3)\delta(x_1-x_4),\end{aligned} \tag{4}$$

where we used Eq.(2) and the fact that $s^{\sigma\bar{\sigma}}_a = G^{aa}_{\sigma\bar{\sigma}}(x, x+0^-)$ [1].

Let us now define the physical susceptibility in the transverse-spin channel:

$$\chi^{ab}_{\sigma\bar{\sigma}}(x_1,x_2) = T_\tau \left\langle S^{\sigma\bar{\sigma}}_a(x_1) S^{\bar{\sigma}\sigma}_b(x_2)\right\rangle , \tag{5}$$

where $S^{\sigma\sigma'}_a(x) = e^{H\tau} c^\dagger_{ia\sigma} c_{ia\sigma'} e^{-H\tau}$, with $x = (R_i, \tau)$. Since the vertex function in Eq.(2) is local and static, the BSE (see Appendix D for the derivation) for the physical susceptibilities is similar to the one obtained in RPA [17] and reads:

$$\bar{\bar{\chi}}^{-1}_{\overline{\sigma\bar{\sigma}}}(q) = \bar{\bar{\chi}}^{-1}_{0,\overline{\sigma\bar{\sigma}}}(q) + \bar{\bar{\Gamma}}_{\overline{\sigma\bar{\sigma}}}, \tag{6}$$

where we used the double bar to indicate 2×2 matrices, $q = (i\omega_n, \mathbf{q})$ with $\omega_n = 2\pi n/\beta$ and $\mathbf{q}$ being respectively the bosonic Matsubara frequency and crystalline exchanged momentum, $\bar{\bar{\chi}}_{\overline{\sigma\bar{\sigma}}}(q)$ is given by the Fourier transform of the susceptibility defined in Eq.(5), $\bar{\bar{\Gamma}}_{\overline{\sigma\bar{\sigma}}} = -\lambda U\, \mathbb{I}_{2\times2}$ and $\chi^{ab}_{0,\overline{\sigma\bar{\sigma}}} = -\frac{1}{V\beta}\sum_k G^{ab}_\sigma(k) G^{ab}_{\bar{\sigma}}(k+q)$. The Green's function is obtained using the Dyson equation and reads:

$$\bar{\bar{G}}^{-1}_\sigma(k) = \epsilon_{\mathbf{k}}\,\sigma^x + [i\nu + \mu - \frac{\Gamma_{\overline{\uparrow\downarrow}}}{2}(n+\sigma m)]\mathbb{I}_{2\times2}, \tag{7}$$

[1] We used the overline symbol, i.e. $\overline{\uparrow\downarrow}$, to distinguish this vertex component from those belonging to the longitudinal spin channel, that are defined in the next paragraphs.

where n is the electron density and $m = n_{A\uparrow} - n_{A\downarrow}$ is the staggered magnetisation.

In order to univocally determine single-particle and two-particle properties, we have to solve a set of self-consistent equations that will allow us to find the chemical potential, staggered magnetization and double occupancies (μ, m, $\langle \hat{n}_\uparrow \hat{n}_\downarrow \rangle$) as a function of the electron density, on-site interaction and temperature. In this work we will specialize in the case of the three-dimensional cubic lattice at half-filling , i.e. $n = 1$, that corresponds to fixing the chemical potential to $\mu = \frac{\Gamma_{\overline{\uparrow\downarrow}}}{2}$.

Since the self-energy is static and local, the gap equation for the order parameter is similar to the one obtained in mean-field theory and is given by following expression:

$$\frac{1}{(2\pi)^3} \int_{BZ} d\mathbf{k} \, \frac{|\Gamma_{\overline{\uparrow\downarrow}}|}{2E_{\mathbf{k}}} \tanh\left(\frac{\beta E_{\mathbf{k}}}{2}\right) = 1, \tag{8}$$

where $E_{\mathbf{k}} = \sqrt{\epsilon_{\mathbf{k}}^2 + \left(\frac{m\Gamma_{\overline{\uparrow\downarrow}}}{2}\right)^2}$, with $\epsilon_{\mathbf{k}} = -2t\left[\cos(k_x) + \cos(k_y) + \cos(k_z)\right]$. Differently from mean-field theory however, the order parameter is not univocally determined by the gap equation, because the double occupancies, appearing in Eq.(8), are still unknown.

As a direct consequence of its definition in Eq.(5), the susceptibility in the transverse channel assumes the following limiting value $\sum_\sigma \chi^{aa}_{\sigma\bar{\sigma}}(x, x + 0^-) = n - 2\langle \hat{n}_\uparrow \hat{n}_\downarrow \rangle$, which implies the following sum rule for its Fourier transform:

$$\frac{1}{\beta(2\pi)^3} \sum_{\omega_n \sigma} \int_{\mathrm{BZ}} d\mathbf{q} \, \chi^{aa}_{\sigma\bar{\sigma}}(q) = n - 2\langle \hat{n}_\uparrow \hat{n}_\downarrow \rangle . \tag{9}$$

Hence, Eqs.(8,9) provide with a closed set of equations that must be solved self-consistently in order to determine the order parameter and the double occupancies.

3.2 Spin-longitudinal channel

The irreducible vertex function in the longitudinal-spin channel reads:

$$\begin{aligned}\Gamma^{abcd}_{\sigma\sigma'}(x_1, x_2, x_3, x_4) &= \frac{\delta\Sigma^{ba}_{\sigma\sigma}(x_2, x_1)}{\delta G^{cd}_{\sigma'\sigma'}(x_3, x_4)} \\ &\sim U_{\sigma\sigma'}\delta_{\sigma\bar{\sigma}'}\delta_{ab}\delta_{ac}\delta_{ad}\,\delta(x_1 - x_2)\delta(x_1 - x_3)\delta(x_1 - x_4).\end{aligned} \tag{10}$$

Differently from Eq.(4) which is an exact equality, a further approximation, similar to the one performed in the charge channel in the paramagnetic phase [21, 24], is needed to write Eq.(10) in its final form (see Appendix B).

Let us define the susceptibilities in the spin-longitudinal channel:

$$\chi^{ab}_{\sigma\sigma'}(x_1, x_2) = T_\tau \langle n_{a\sigma}(x_1) n_{b\sigma'}(x_2) \rangle - \langle n_{a\sigma} \rangle \langle n_{b\sigma'} \rangle \tag{11}$$

Given the local and static form of the vertex function in Eq.(10), the expression of the susceptibilities in the charge and spin-longitudinal channel, in presence of particle-hole symmetry [2], can be written as following:

$$\chi_z(q) = \frac{\chi_{0,\|}(q)}{1 - \Gamma_z \chi_{0,\|}(q)} \tag{12}$$

$$\chi_\rho(q) = \frac{\chi_{0,\|}(q)}{1 + \Gamma_\rho \chi_{0,\|}(q)}, \tag{13}$$

where $\chi_z = \frac{1}{2}\sum_{ab\sigma\sigma'}(-1)^{a+b+\sigma+\sigma'}\chi^{ab}_{\sigma\sigma'}$, $\chi_\rho = \frac{1}{2}\sum_{ab\sigma\sigma'}\chi^{ab}_{\sigma\sigma'}$, $\Gamma_z = \frac{1}{2}\sum_{\sigma\sigma'}(-1)^{\sigma+\sigma'}\Gamma_{\sigma\sigma'}$, $\Gamma_\rho = \frac{1}{2}\sum_{\sigma\sigma'}\Gamma_{\sigma\sigma'}$, $\chi_{0,\|} = -\frac{1}{2V\beta}\sum_{k\sigma b} G^{Ab}_\sigma(k) G^{bA}_\sigma(k+q)$. Analogously for the spin-transverse channel, we can determine the value of the vertices Γ_z and Γ_ρ by imposing the following sum rule for the longitudinal channel susceptibilities:

$$\frac{2}{\beta(2\pi)^3}\sum_{\omega_n}\int_{\mathrm{BZ}} d\mathbf{q}\, \chi_z(q) = n - 2\langle \hat{n}_\uparrow \hat{n}_\downarrow\rangle - m^2 \tag{14}$$

$$\frac{2}{\beta(2\pi)^3}\sum_{\omega_n}\int_{\mathrm{BZ}} d\mathbf{q}\, \chi_\rho(q) = n + 2\langle \hat{n}_\uparrow \hat{n}_\downarrow\rangle - n^2. \tag{15}$$

Since Eqs.(8,9) are a set of closed equations, Eqs.(14,15) can be solved separately once the values of m and $\langle \hat{n}_\uparrow \hat{n}_\downarrow\rangle$ have been self-consitently obtained from the spin-transverse channel.

3.3 Improved one-loop self-energy

In TPSC it is possible to obtain an improved self-energy that, differently from the one appearing in Eq.(2), depends on both momenta and frequency. This can be achieved by computing the TPSC vertices and susceptbilities and using them as input for the equation of motion [22, 38]. Extending this procedure to the broken symmetry phase we obtain the following expression for the improved self-energy:

$$\begin{aligned}\Sigma^{ab}_\sigma(k) - U n_{a\bar{\sigma}} = &-\frac{U}{2V\beta}\sum_q G^{ab}_{\bar{\sigma}}(k+q)\Gamma^{a}_{\sigma\bar{\sigma}\overline{\sigma\bar{\sigma}}}\chi^{ab}_{\overline{\sigma\bar{\sigma}}}(q) \\ &+\frac{U}{2V\beta}\sum_{q\sigma_1} G^{ab}_{\sigma}(k+q)\Gamma^{a}_{\sigma\sigma_1}\chi^{ab}_{\sigma_1\bar{\sigma}}(q),\end{aligned} \tag{16}$$

where $G^{ab}_\sigma(k)$ is given by Eq.(7). In appendix E we show the derivation of Eq.(16).

4 Numerical results

Fig. (1-a) shows the order parameter as a function of temperature for different values of the on-site interaction. The order parameter decreases as a function of increasing temperature until it vanishes at the critical temperature. Close to the phase transition, the order parameter behaves like $m = \alpha|T - T_c|^\beta$ with critical exponent $\beta = 1/2$, which is consistent with the universality class of the spherical model [23, 39]. In Fig.(1-b), we show the value of the vertex renormalisation $\lambda = |\Gamma_{\overline{\uparrow\downarrow}}|/U$ as a function of temperature for different values of U. We observe

[2]In general, the charge and longitudinal-spin channels interact via a mixed terms $\chi_{\bar{z}\rho}$ [36, 37] that vanishes only in presence of particle-hole symmetry [17]

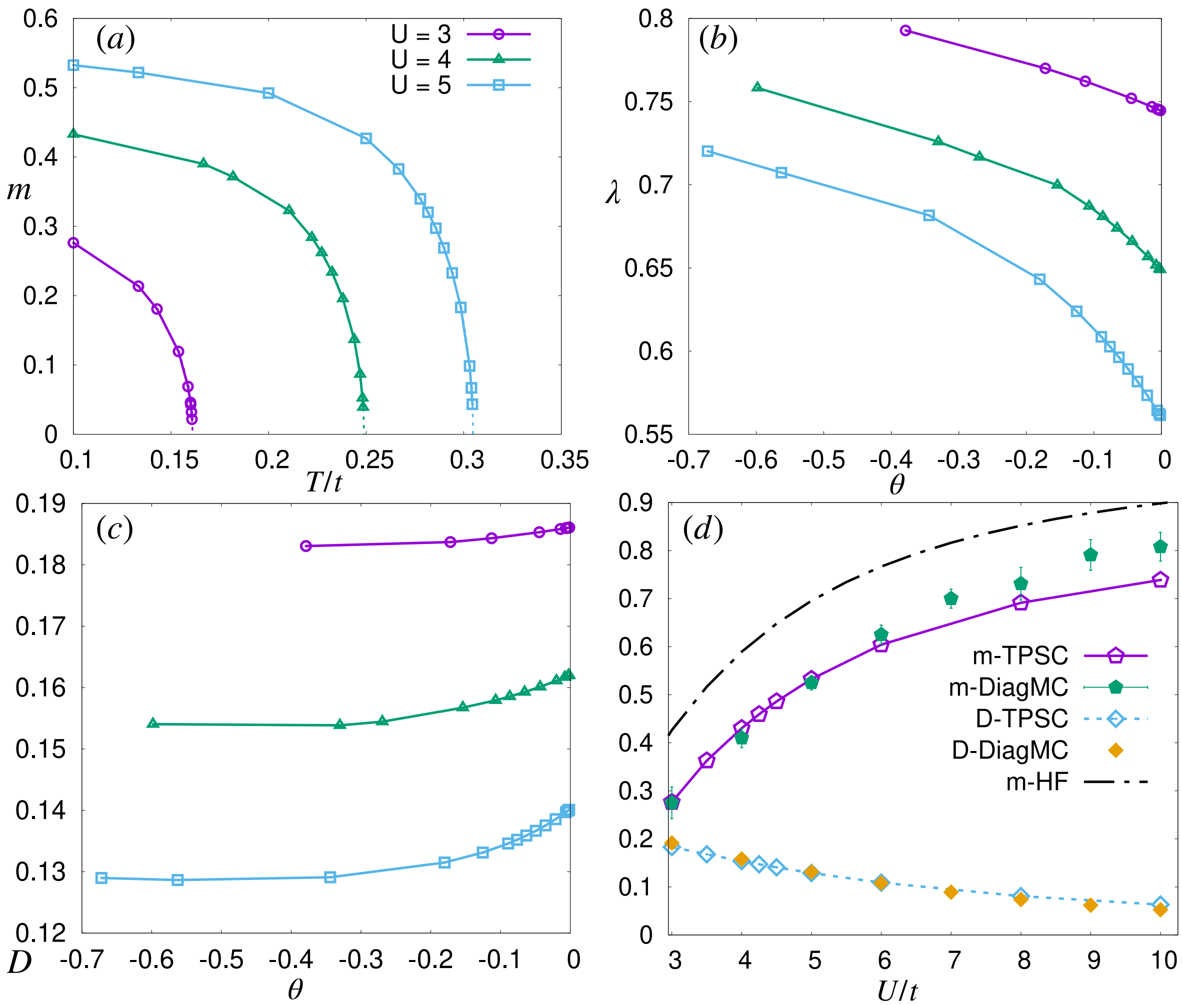

Figure 1: (a) Staggered magnetisation m as a function of T for three different values of $U/t = 3, 4, 5$. Dashed lines are best fits of the function $\alpha|T - T_c|^{1/2}$ close to T_c. (b) λ parameter as a function of the reduced temperature $\theta = \frac{T-T_c}{T_c}$ for the three different values of the on-site interaction. (c) Double occupancies $D = \langle \hat{n}_\uparrow \hat{n}_\downarrow \rangle$ as a function of θ for the three different U values. (d) Magnetisation and double occupancies as a function of U for $T/t = 1/10$. TPSC data (open symbols) are compared to the DiagMC results (filled symbols) adapted from Ref. [13]. The black dashed line is the magnetisation curve obtained using Hartree-Fock.

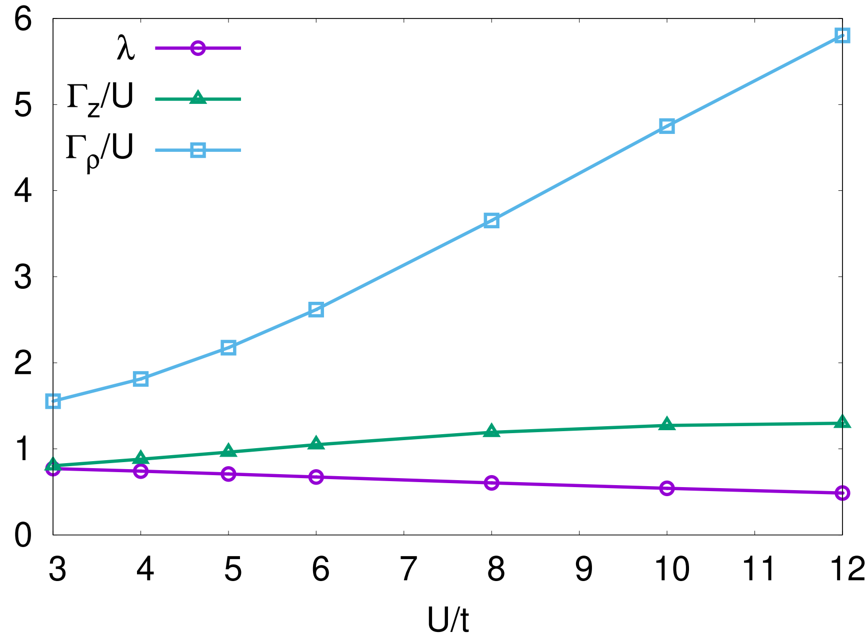

Figure 2: Vertex renormalisations in the density (Γ_ρ/U), spin-longitudinal (Γ_z/U) and spin transverse ($\lambda = |\Gamma_{\overline{\uparrow\downarrow}}|/U$) channels as a function of the bare interaction for $T/t = 1/7.5$.

that λ decreases as a function of increasing interactions, as expected, since the system get more correlated when U increases. On the other hand, λ increases by decreasing the temperature from the critical one, which can be rationalised in the following way: when symmetry breaking is allowed, the system can reduce the number of double occupancies $\langle \hat{n}_\uparrow \hat{n}_\downarrow \rangle = \frac{\lambda}{4}(n^2 - m^2)$, shown in Fig.(1-c), (and therefore minimize the potential energy) by increasing the order parameter, rather than by decreasing λ. Hence, our results show that the degree of correlation of the system is reduced deep in the broken symmetry phase far away from the the critical temperature.

In Fig.(1-d), we show the order parameter and double occupancies as a function of U by fixing the temperature to $T/t = 1/10$. As expected we observe that the order parameter (double occupancies) increases (decrease) as a function of U. It is worth to highlight that the introduction of quantum fluctuations leads to a significant decrease in the staggered magnetization compared to its mean-field predicted value [black curve in Fig. (1-d)]. We compared our results to the ones obtained using Monte Carlo in Ref. [13] and we observe an excellent quantitative agreement.

After solving Eqs.(8,9) we can use the values of double occupations and staggered magnetisation as input for Eqs.(14,15) in order to obtain the renormalised vertices in the longitudinal channel. In Fig.(2), we show the renormalisation factors of the vertices, i.e. Γ_ρ/U, Γ_z/U and λ as a function of U for $T/t = 1/7.5$. We observe that Γ_ρ is highly enhanced with respect to the bare vertex which is similar to what has been already observed in the paramagnetic phase of the Hubbard model using TPSC [22]. Differently from the symmetric case, in the AF phase $\Gamma_z \neq |\Gamma_{\overline{\uparrow\downarrow}}|$, and our results show that $\Gamma_z > |\Gamma_{\overline{\uparrow\downarrow}}|$ for all values of U and that the difference between the two vertices increases as a function of the on-site interaction. Interestingly, while $|\Gamma_{\overline{\uparrow\downarrow}}|$ is always lower than the bare vertex (as U_s in the paramagnetic phase [22]), this is not true anymore for Γ_z/U, which is also an increasing function of U and crosses the unity at $U/t \sim 5.4$ for $T/t = 1/7.5$ [see Figure 2].

In Appendix C we describe how the integral appearing in Eq.(9) has been numerically evaluated.

4.1 Dynamical Susceptibilities

We can use the solution of the self-consistent equations to evaluate spectral properties of two-particle propagators. Regarding the spin-transverse channel, we observe that self-energy and vertex corrections are both controlled by the same quantity, i.e. $\Gamma_{\overline{\uparrow\downarrow}}$, which substitutes *de facto* the bare vertex appearing in RPA. Therefore, the spin-transverse dynamical susceptibility defined in Eq.(6), which contains the information about the Goldstone modes, calculated at a given U corresponds to the RPA one evaluated at a lower value of the interaction, namely $|\Gamma_{\overline{\uparrow\downarrow}}(U)|$.

Conversely, the vertex in the spin-longitudinal susceptibility Γ_z assumes different values than $\Gamma_{\overline{\uparrow\downarrow}}$ because of symmetry breaking, and $\Gamma_z > |\Gamma_{\overline{\uparrow\downarrow}}|$ as shown in Figure 2. This implies that the spin-longitudinal susceptibility evaluated in TPSC does not correspond to any RPA one evaluated at different effective parameters, and consequently the two methods yield qualitatively different results for the spin-longitudinal susceptibility. In particular, since $\Gamma_z > |\Gamma_{\overline{\uparrow\downarrow}}|$ the gap in the χ_z spectrum is reduced with respect to the quasi-particle gap predicted by TPSC, i.e. $2\Delta_{\rm TPSC} = |\Gamma_{\overline{\uparrow\downarrow}}|\, m$, which is controlled by self-energy corrections. In Fig.(3-a) we show a color plot of $\mathrm{Im}\chi_z(q)$ that has been evaluated in the high-symmetry path of the BZ and for a wide range of frequencies at $U/t = 12$ and $T/t = 1/7.5$. We observe that a well visible Higgs mode appears well below the quasi-particle continuum starting at $2\Delta_{\rm TPSC}$, it has a minimum at $R = (\pi, \pi, \pi)$, and presents a substantial dispersion along the M-R and R-Γ directions. This is in stark contrast with the RPA predicted spectrum [shown in Fig.(3-b)], where the Higgs resonance occurs at $\omega/t = 2\Delta_{\rm HF}$ and therefore is overdamped by the particle-hole continuum [40, 41]. Our findings agree qualitatively with recent numerical results based on a time-dependent Gutzwiller approach showing that the Higgs resonance is shifted below the edge of the particle-hole continuum upon increasing the interaction [42]. In Figs.(3-c/d) we show $\mathrm{Im}\chi_z$ evluated using TPSC and RPA as a function of the real frequencies for a fixed momentum close to R and two values of the interactions $U/t = 12, 5$ and at $T/t = 1/7.5$. It is apparent that for both values of the interaction the Higgs resonance predicted by TPSC is well separated from the particle-hole continuum and occurs at lower energies, while RPA does not yield any true isolated pole.

5 Conclusions

We extended the formalism of TPSC to the case of spontaneous symmetry breaking and employed the new method to the AF phase of the single band Hubbard model in the cubic lattice at half-filling. Our comparison with DiagMC shows an excellent quantitative agreement between the two methods for the order parameter and double occupancies.

We show that the differentiation of vertex corrections in the different scattering channels due to symmetry breaking ($\Gamma_z \neq |\Gamma_{\overline{\uparrow\downarrow}}|$) has remarkable effects in the spin-longitudinal channel. In particular, the Higgs resonance occurs at energies lower than the quasi-particle continuum leading to a well visible Higgs mode for a wide range of parameters.

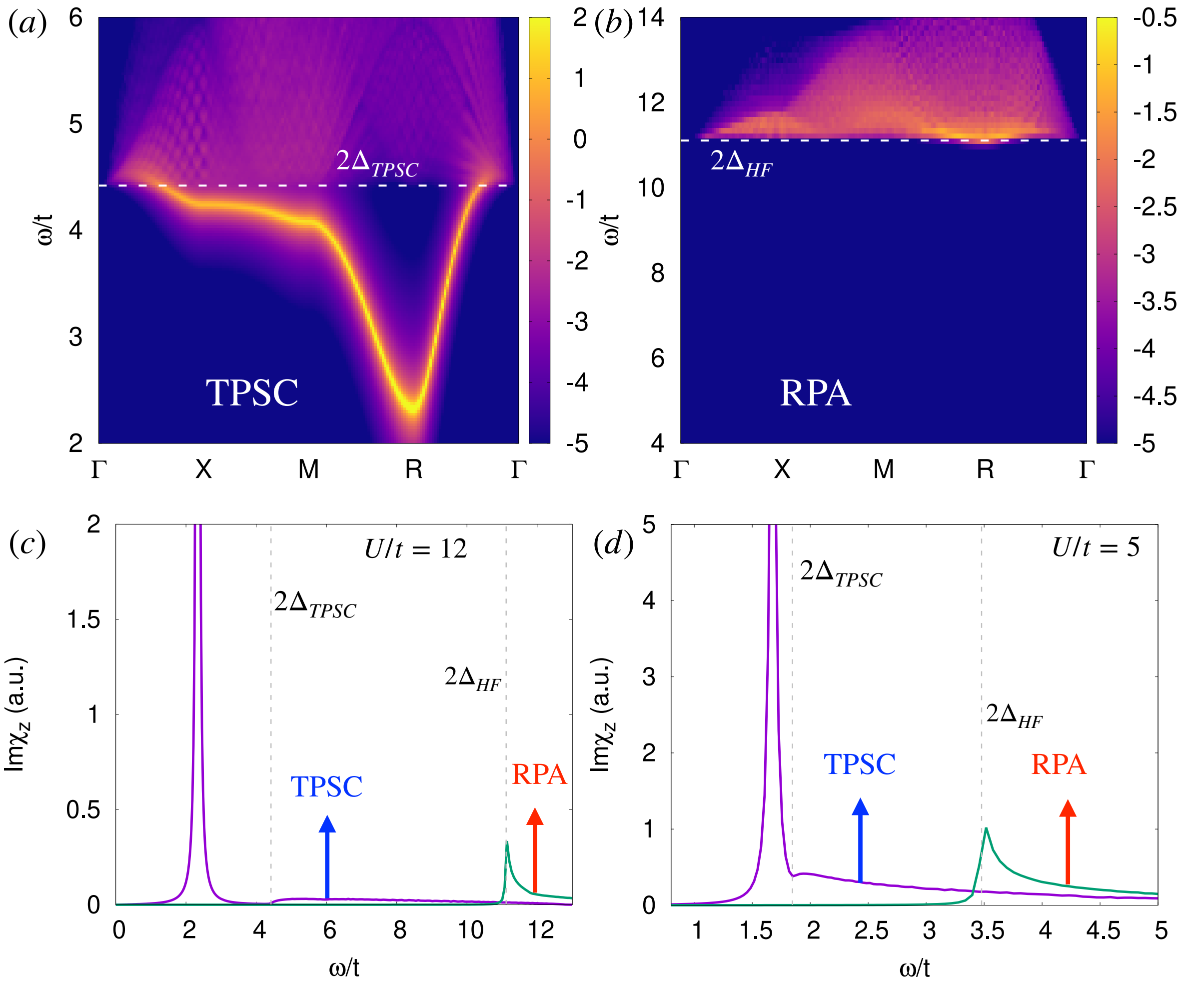

Figure 3: (a) Imaginary part of $\chi_z(\omega + i\eta, \mathbf{q})$ (in log scale) defined in Eq.(12) evaluated along the BZ high-symmetry path and for a wide range of real frequencies, for $U/t = 12$, $T/t = 1/7.5$, and $\eta/t = 0.03$. (b) Imaginary part of $\chi_z(\omega + i\eta, \mathbf{q})$ (in log scale) calculated using RPA for for $U/t = 12$, $T/t = 1/7.5$, and $\eta/t = 0.02$. (c) $\mathrm{Im}\chi_z(\omega + i\eta, \mathbf{q})$ evaluated using TPSC and RPA at fixed momentum $\mathbf{q} = (\pi, \pi, \pi + 0.1)$ at $U/t = 12$, $T/t = 1/7.5$ and for $\eta = 0.03$. (d) Same as (c) but for $U/t = 5$.

Since our data demonstrate that the level of correlation decreases by decreasing temperature deep in the BSP, one could argue that TPSC is particularly suited to the study of BSP where correlation are not negligible but less pronounced.

The formalism that we developed is generic and could be adapted to more complicated multi-band models and open the possibility for efficient treatment of correlation effects in realistic materials in BSP. Also, since TPSC already has been used as a benchmark for cold atomic simulators [43, 44], its generalisation will provide further guidance to cold-atom experiments exploring broken symmetry phases [45].

Generalising improved version of TPSC such as TPSC+ and TPSC+SFM [28] to the BSP case could lead to the partial inclusion of dynamical effects, which have been shown to be particularly important close to the Neél temperature [46, 47], and is left to future work.

Acknowledgment

I thank Walter Metzner, Alessandro Toschi, Georg Rohringer, Thomas Schäfer and Lara Benfatto for valuable discussions. I also thank Renaud Garioud for providing the DiagMC data.

A Equation of motion and TPSC ansatz

Let us introduce the generalised multi-flavor indices α, which for example coincide with $\alpha = (a, \sigma)$ containing both sub-lattice (a) and spin (σ) indices in the AF or to spin indices in the FM case. Then, we can rewrite the Hubbard hamiltonian in the following form:

$$H = \sum_{\langle ij \rangle} \sum_{\alpha\beta} c^\dagger_{i\alpha} \mathcal{H}^{\alpha\beta} c_{j\beta} + \frac{1}{2} \sum_{i} \sum_{\alpha\beta} U_{\alpha\beta}\, \hat{n}_{i\alpha} \hat{n}_{i\beta}. \tag{17}$$

In the case of FM, we have that $\mathcal{H}^{\alpha\beta} = -t\delta_{\alpha\beta}$ and $U_{\alpha\beta} = \delta_{\alpha\bar{\beta}} U$, whereas for the AF case we have $\mathcal{H}^{\alpha\beta} = -t\delta_{\sigma\sigma'}\delta_{a\bar{b}}$ and $U_{\alpha\beta} = \delta_{\sigma\bar{\sigma}'}\delta_{ab} U$.

Let us define the electronic Green's function as $G^{\alpha\beta}(x, y) = -T_t \left\langle c_\alpha(x) c^\dagger_\beta(y) \right\rangle$, where $x = (R_i, \tau_i)$ is a four-vector containing the lattice coordinate R_i and the imaginary time τ_i, and $c_\alpha(x) = e^{H\tau_i} c_{i\alpha} e^{-H\tau_i}$. Then, the equation of motion of the Green's function reads:

$$\begin{aligned} \partial_{\tau_i} G^{\alpha\beta}(x, y) = \delta_{\alpha\beta}\delta(x - y) - \mathcal{H}^{\alpha\gamma}(x, \overline{y}) G^{\gamma\beta}(\overline{y}, y) \\ - U_{\alpha\gamma} G^{(2)\beta\alpha}_{\ \ \gamma\gamma}(y, x + 0^-, x + 0^+, x), \end{aligned} \tag{18}$$

where a summation over repeated indices is intended, $\mathcal{H}^{\alpha\gamma}(x, y) = \mathcal{H}^{\alpha\beta}_{ij}\delta(\tau_i - \tau_j)$, and $G^{(2)}$ is the two-particle Green's function, that is defined as following:

$$G^{(2)\alpha\beta}_{\ \ \gamma\delta}(x_1, x_2, x_3, x_4) = T_\tau \left\langle c^\dagger_\alpha(x_1) c_\beta(x_2) c^\dagger_\gamma(x_3) c_\delta(x_4) \right\rangle.$$

Let us introduce the self-energy Σ through the Dyson's equation:

$$\begin{aligned} \Sigma^{\alpha\gamma}(x, \overline{y}) G^{\gamma,\beta}(\overline{y}, y) = G_0^{-1\,\alpha\gamma}(x, \overline{y}) G^{\gamma\beta}(\overline{y}, y) \\ + \delta_{\alpha\beta}\delta(x - y). \end{aligned} \tag{19}$$

If we substitute the last equation into Eq.(18), we obtain the equation of motion in the following form:

$$\Sigma^{\alpha\gamma}(x,\overline{y})G^{\gamma,\beta}(\overline{y},y) = U_{\alpha\gamma}G^{(2)\beta\alpha}_{\gamma\gamma}(y,x+0^-,x+0^+,x). \tag{20}$$

Due to the presence of $G^{(2)}$, Eq.(20) is not closed for the self-energy and single-particle Green's, and in order to obtain an explicit expression for Σ further approximations must be carried on. In mean-field theory the two-particle Green's function is replaced by its disconnected part, that is a valid approximation only at weak coupling. In TPSC [21, 22, 24, 25], in order to take into account of correlation effects, and at the same time to reduce the complexity of Eq.(20), the following assumption is considered:

$$\Sigma^{\alpha\gamma}(x,\overline{y})G^{\gamma,\beta}(\overline{y},y) \sim \lambda^{\alpha\gamma}\,U_{\alpha\gamma}\left[G^{\alpha\beta}(x,y)n_\gamma - s^{\alpha\gamma}G^{\gamma\beta}(x,y)\right], \tag{21}$$

where $n_\alpha = \langle\hat{n}_{i\alpha}\rangle$, $s^{\alpha\beta} = \left\langle c^\dagger_{i\beta}c_{i\alpha}\right\rangle$, and $\lambda^{\alpha\beta}$ is an extra-coefficient that must be determined self-consistently and contains correlation effects. When $\lambda^{\alpha\beta} = 1$ mean-field theory is recovered. The parameter λ can be determined by requiring that the equal-time/position limit of Eq.(20), i.e. $y = x + 0^{++}$, is preserved exactly when $\beta = \alpha$ [3], by imposing:

$$\lambda^{\alpha\gamma} = \frac{\langle\hat{n}_\alpha\,\hat{n}_\gamma\rangle}{n_\alpha n_\gamma - s^{\alpha\gamma}s^{\alpha\gamma}}\;. \tag{22}$$

From Eq.(20), we can isolate the self-energy that reads:

$$\Sigma^{\alpha\beta}(x-y) = \delta(x-y)\left(\delta_{\alpha\beta}\lambda^{\alpha\gamma}U_{\alpha\gamma}n_\gamma - \lambda^{\alpha\beta}U_{\alpha\beta}s^{\alpha\beta}\right). \tag{23}$$

In the FM/AF phase of the Hubbard model, the expression for the λ parameter simplifies as following:

$$\lambda = \frac{\langle\hat{n}_\uparrow\hat{n}_\downarrow\rangle}{n_\uparrow n_\downarrow}, \tag{24}$$

which is identical to the one in the paramagnetic case [22, 24]. Since in the FM/AF phase Eq.(24) does not depend on the spin/sub-lattice indices, we omitted those indices in the expression of λ, and therefore we need to optimize only one parameter even within the broken-symmetry phases under scrutiny. Hence, in the AF phase the expression of the self-energy can be written as:

$$\Sigma^{ab}_{\sigma\sigma'}(x,y) = \delta(x-y)\delta_{ab}U_{\overline{\uparrow\downarrow}}\left(\delta_{\sigma\sigma'}n_{a\bar{\sigma}} - \delta_{\sigma\bar{\sigma}'}s^{\sigma\bar{\sigma}}_a\right), \tag{25}$$

where $U_{\overline{\uparrow\downarrow}} = \lambda U$, a, b are sub-lattice indices. We notice that in a AF phase the components of the self-energy off-diagonal in the spin indices should vanish, i.e. $s^{\sigma\bar{\sigma}} = 0$. However, it is useful to keep those terms in the expression of the self-energy for the derivation of the Bethe-Salpeter equation in the spin-transverse channel. Therefore, we will consider the presence of an external field that breaks spin-conservation and eventually compute the functional derivatives of Σ with respect to the off-diagonal component of the propagator in the limit of a vanishing field.

[3]In the case of the AF phase that we address in this work, spin conservation implies that $\langle c^\dagger_\alpha\hat{n}_\gamma c_\beta\rangle = 0$ at zero field. when $\alpha \neq \beta$, and therefore we shall introduce the λ-correction only for the two-particle Green's functions that do not vanish in the limit of zero external field.

B Irreducible vertices

In this section we shall give some details about the derivation of the expression for the irreducible vertices in the spin-transverse and spin-longitudinal channels.

B.1 Spin-transverse channel

It is worth to note that the expression for the irreducible vertex in the spin-transverse channel presented in the main text is an exact equality. In fact, even if λ is a functional of the Green's function, it does not appear in the expression of the irreducible vertex function because its functional derivative with respect to the off-diagonal propagator vanishes, i.e.

$$\frac{\delta\lambda}{\delta G^{cd}_{\downarrow\uparrow}(x_3,x_4)} = 0. \tag{26}$$

In fact, from Eq.(20) we can derive the following formula for the double occupancies:

$$\langle \hat{n}_{a\sigma}\hat{n}_{a\bar{\sigma}}\rangle = \frac{1}{2U}\Sigma^{aa'}_{\sigma\sigma'}(x,\overline{y})G^{a'a}_{\sigma'\sigma}(\overline{y},x). \tag{27}$$

Let us now compute the functional derivative of the double occupancies:

$$\begin{aligned}\frac{\delta\langle \hat{n}_{a\uparrow}\hat{n}_{a\downarrow}\rangle}{\delta G^{\downarrow\uparrow}_{cd}(x_3,x_4)} \propto \delta(x-x_4)\delta_{ad}\Sigma^{\uparrow\downarrow}_{dc}(x_4,x_3)+ \\ \frac{\delta\Sigma^{\uparrow\sigma'}_{aa'}(x,\overline{y})}{\delta G^{\downarrow\uparrow}_{cd}(x_3,x_4)}G^{\sigma'\uparrow}_{a'a}(\overline{y},x),\end{aligned} \tag{28}$$

where we can now easily see that the LHS does not conserve the spin along the z-axis and therefore vanishes at zero external field.

B.2 Spin-longitudinal channel

On the other hand the expression for the irreducible vertex in the spin-longitudinal channel given in the main text is not an exact equality. Here we shall clarify where the extra approximation comes from. The irreducible vertex function in the longitudinal-spin channel reads:

$$\begin{aligned}\Gamma^{abcd}_{\sigma\sigma'}(x_1,x_2,x_3,x_4) &= \frac{\delta\Sigma^{ab}_{\sigma\sigma}(x_2,x_1)}{\delta G^{cd}_{\sigma'\sigma'}(x_3,x_4)} \\ &= U_{\overline{\uparrow\downarrow}}\delta_{\sigma\bar{\sigma}'}\delta_{ab}\delta_{ac}\delta_{ad}\delta(x_1-x_2)\delta(x_1-x_3)\delta(x_1-x_4) \\ &+ U\,n_{a\bar{\sigma}}\,\delta(x_1-x_2)\delta_{ab}\frac{\delta\lambda}{\delta G^{cd}_{\sigma'\sigma'}(x_3,x_4)}.\end{aligned} \tag{29}$$

Therefore, the irreducible vertex in the spin-longitudinal channel acquires non-local and dynamical corrections, which would complicate the expression of the Bethe-Salpeter equations and further approximations are needed. In practice, one approximates the extra dynamical term to a constant deviation from the value obtained in the spin-transeverse channel, i.e. $\Gamma_{\rho/z} \sim -\Gamma_{\overline{\uparrow\downarrow}} + \delta U_{\rho/z}$.

C Numerical evaluation of integrals

Integrals in the Brillouin zone have been numerically calculated employing the trapezoidal rule in three dimensions and using grids of $N_k \times N_k \times N_k$ points with N_k up to 32. A particular numerical strategy has been employed for the numerical integration of the spin-transverse susceptibility evaluated at zero frequency, i.e. $\int d\mathbf{q} \sum_\sigma \chi_{\sigma\bar{\sigma}}(\mathbf{q}, 0)$. In fact, since this function diverges at $\mathbf{q} = \mathbf{\Pi}$, we have excluded that point from the grid of integration. We evaluated the integral for different values of $N_k = 21, 24, 28, 32$ and then we extrapolated the integral value by fitting the function $I + h/N_k$, where I is the extrapolated value.

D Bethe-Salpeter Equations

Let us define the generalized susceptibility as:

$$\chi_{1234} = \frac{\delta G(21)}{\delta h(34)}, \tag{30}$$

where $G(12) = -T_\tau \left\langle c_\alpha(x_1) c^\dagger_\beta(x_2) \right\rangle$ is the propagator, $x = (R, \tau)$, $1 = (\alpha, x_1)$ and $h(12)$ is the perturbing field whose action reads:

$$S_{\text{ext}} = -\int d1d2\, h(1,2)\, \bar{c}(1) c(2), \tag{31}$$

where in the last equations c and $\bar{c}$ are Grassmann variables, and$\int d1 = \sum_\alpha \sum_R \int_0^\beta d\tau$, with $\beta = 1/k_B T$. Given the form of the external perturbation, the inverse of the non-interacting propagator reads:

$$\mathcal{G}_0^{-1}(12) = [\partial_\tau + \mu - H_0]_{12} + h(12). \tag{32}$$

We now want to obtain a closed equation for χ_{1234} by explicitly performing the functional derivative in Eq.(30). For doing so we first note that:

$$\frac{\delta G(21)}{\delta h(34)} = -\int\int d1'd2'\, G(2,2') \frac{\delta G^{-1}(2'1')}{\delta h(34)}\, G(1',1). \tag{33}$$

We can further develop Eq.(33) by making use of the Dyson equation, that reads:

$$G^{-1}(12) = \mathcal{G}_0^{-1}(12) - \Sigma(12). \tag{34}$$

In fact, by substituting Eq.(34) into Eq.(33) and using Eq.(32), we obtain the following identity:

$$\begin{aligned}\chi_{1234} = &-G(2,3)G(4,1) \\ &+ \int \prod_{i=1}^{4} di' G(2,2')G(1',1)\Gamma_{1'2'3'4'}\chi_{4'3'34},\end{aligned} \tag{35}$$

where we defined the two-particle irreducible (2PI) vertex function $\Gamma_{1234} = \frac{\delta\Sigma(2,1)}{\delta G(3,4)}$. Let us express the last equation in Fourier space. For this purpose let us expand the propagators and vertices in terms of their Fourier components, i.e.:

$$
\begin{aligned}
f_{1234} &= \frac{1}{(V\beta)^3}\sum_{kk'q} e^{i[kx_1-(k+q)x_2+(k'+q)x_3-k'x_4]} f^{\alpha\beta}_{\gamma\delta}(k,k',q), \\
G(1,2) &= \frac{1}{V\beta}\sum_k e^{-ik(x_1-x_2)} G^{\alpha\beta}_k\,.
\end{aligned}
\tag{36}
$$

We first note that:

$$
\begin{aligned}
-G(2,3)G(4,1) = \frac{1}{(V\beta)^3}&\sum_{kk'q} e^{i[kx_1-(k+q)x_2+(k'+q)x_3-k'x_4]} \\
&\times \chi^{\alpha\beta}_{0,\gamma\delta}(k,k',q),
\end{aligned}
\tag{37}
$$

where we defined the bubble terms as:

$$
\chi^{\alpha\beta}_{0,\gamma\delta}(k,k',q) = -(V\beta)\,\delta_{kk'}\,G^{\delta\alpha}_k\,G^{\beta\gamma}_{k+q}. \tag{38}
$$

The final equation in Fourier space reads:

$$
\chi^{\alpha\beta}_{\gamma\delta}(kk'q) = \chi^{\alpha\beta}_{0,\gamma\delta}(k,k',q) - \frac{1}{(V\beta)^2}\sum_{k_1k_2}\sum_{\alpha'\beta'\gamma'\delta'} \chi^{\alpha\ \beta}_{0,\beta'\alpha'}(k,k_1,q)\,\Gamma^{\alpha'\beta'}_{\gamma'\delta'}(k_1,k_2,q)\,\chi^{\delta'\gamma'}_{\gamma\ \delta}(k_2,k',q)\,. \tag{39}
$$

E Improved one-loop self-energy

Let us note that from its definition the generalised susceptiblity is related to the two-particle Green's function in the following way: $\chi^{\alpha\beta}_{\gamma\delta}(x_1,x_2,x_3,x_4) = G^{(2)\alpha\beta}_{\ \ \ \ \gamma\delta}(x_1,x_2,x_3,x_4) - G^{\beta\alpha}(x_2,x_1)G^{\delta\gamma}(x_4,x_3)$. Hence, we can rewrite the RHS of Eq.(18) in the following way:

$$
\begin{aligned}
&\frac{1}{V\beta}\sum_{k\gamma} e^{-ik(x-y)}U_{\alpha\gamma}n_\gamma G^{\alpha\beta}_k \\
&+ \frac{1}{(\beta V)^3}\sum_{kk'q}\sum_{\gamma} U_{\alpha\gamma}e^{-ik(x-y)}\chi^{\alpha\beta}_{\gamma\gamma}(kk'q).
\end{aligned}
\tag{40}
$$

If we substitute Eq.(39) into the second term of last equation we obtain the following expression:

$$
\begin{aligned}
&-\frac{1}{(V\beta)^2}\sum_{kk'q}\sum_{\gamma} e^{ik(x-y)}U_{\alpha\gamma}G^{\gamma\alpha}_k G^{\beta\gamma}_{k+q} \\
&+\frac{1}{(V\beta)^4}\sum_{kk'qk_1}\sum_{\gamma\alpha'\beta'\gamma'\delta'} U_{\alpha\gamma}G^{\alpha'\alpha}_k G^{\beta\beta'}_{k+q}\Gamma^{\alpha'\beta'}_{\gamma'\delta'}(kk_1q) \\
&\qquad\times \chi^{\gamma'\beta'}_{\gamma\gamma}(k_1k'q).
\end{aligned}
\tag{41}
$$

The last equation is quite generic and valid for the exact case. Now we shall specialize to the antiferromagnetic phase of the Hubbard model, and approximate the vertex function to a local

α	(a,σ)
β	(b,σ')
γ	(c,σ'')
α'	(a_1,σ_1)
β'	(a_2,σ_2)
γ'	(a_3,σ_3)
δ'	(a_4,σ_4)

Table 1: Relation between indices expressed in the compact and extended notations.

quantity that does not depend on the crystalline momenta. In order to do so it is useful to explicitly express the spin-orbital indices in sub-lattice and spin indices as shown in Table 1.

Furthemore, if we assum spin-conservation we can express the irreducible vertex function as following:

$$\Gamma^{a_1a_2}_{a_3a_4}\Big|^{\sigma_1\sigma_2}_{\sigma_3\sigma_4} \sim \delta_{a_1a_2}\delta_{a_1a_3}\delta_{a_1a_4}(\Gamma^{a_1}_{\sigma_1\sigma_2}\delta_{\sigma_1\sigma_2}\delta_{\sigma_3\sigma_4} + \Gamma^{a_1}_{\overline{\sigma_1\bar{\sigma}_1}}\delta_{\sigma_1\bar{\sigma}_2}\delta_{\sigma_3\bar{\sigma}_4}\delta_{\sigma_1\sigma_3}), \tag{42}$$

where we used the following notation $\Gamma^{a}_{\sigma\sigma'} = \Gamma^{aa}_{aa}|^{\sigma\sigma}_{\sigma'\sigma'}$ and $\Gamma^{a}_{\overline{\sigma\bar{\sigma}}} = \Gamma^{aa}_{aa}|^{\sigma\bar{\sigma}}_{\bar{\sigma}\sigma}$. Substituting Eq.(42) in Eq.(41) we obtain the following expression for the equation of motion in momentum space:

$$\Sigma^{ab}_{\sigma}(k) - Un_{a\bar{\sigma}} = \frac{U}{(V\beta)^3}\sum_{k_1k'q\sigma_1} G^{ab}_{\sigma}(k+q)\Gamma^{b}_{\sigma\sigma_1}(\nu\nu'\omega)\chi^{ba}_{\sigma_1\bar{\sigma}}(k_1k'q). \tag{43}$$

We notice that in this representation the self-energy is expressed in terms of the longitudinal scattering channel only. It is possible to obtain an equivalent expression where the transverse vertex and susceptibility appear by using the following crossing relation:

$$G^{(2)\beta\alpha}_{\gamma\gamma}(y,x+0^-,x+0^+,x) = -G^{(2)\beta\gamma}_{\gamma\alpha}(y,x,x+0^+,x+0^-). \tag{44}$$

Plugging the last equation into the equation of motion in Eq.(18) and following similar passages to the ones we did for obtaining Eq.(43), we obtain the following expression for the self-energy:

$$\Sigma^{ab}_{\sigma}(k) - Un_{a\bar{\sigma}} = -\frac{U}{(V\beta)^3}\sum_{k_1k'q} G^{ab}_{\bar{\sigma}}(k+q)\Gamma^{a}_{\overline{\sigma\bar{\sigma}}}(\nu\nu'\omega)\chi^{ab}_{\overline{\sigma\bar{\sigma}}}(k_1k'q). \tag{45}$$

In TPSC the irreducible vertices are local and static, i.e. they do not depend on the Mastubara frequencies and further simplification arise. In particular, if we assume static and local vertex functions, if we average Eqs.(43,45) we obtain the following expression for the one-loop improved self-energy:

$$\Sigma^{ab}_{\sigma}(k) - Un_{a\bar{\sigma}} = -\frac{U}{2V\beta}\sum_{q} G^{ab}_{\bar{\sigma}}(k+q)\Gamma^{a}_{\overline{\sigma\bar{\sigma}}}\chi^{ab}_{\overline{\sigma\bar{\sigma}}}(q) + \frac{U}{2V\beta}\sum_{q\sigma_1} G^{ab}_{\sigma}(k+q)\Gamma^{a}_{\sigma\sigma_1}\chi^{ab}_{\sigma_1\bar{\sigma}}(q). \tag{46}$$

References

[1] J. Goldstone, *Field theories with superconductor solutions*, Il Nuovo Cimento (1955-1965) **19**(1), 154 (1961).

[2] Y. Nambu and G. Jona-Lasinio, *Dynamical model of elementary particles based on an analogy with superconductivity. i*, Phys. Rev. **122**, 345 (1961), doi:10.1103/PhysRev.122.345.

[3] J. Goldstone, A. Salam and S. Weinberg, *Broken symmetries*, Phys. Rev. **127**, 965 (1962), doi:10.1103/PhysRev.127.965.

[4] H. Watanabe and H. Murayama, *Unified description of nambu-goldstone bosons without Lorentz invariance*, Phys. Rev. Lett. **108**, 251602 (2012), doi:10.1103/PhysRevLett.108.251602.

[5] H. Watanabe and H. Murayama, *Effective lagrangian for nonrelativistic systems*, Phys. Rev. X **4**, 031057 (2014), doi:10.1103/PhysRevX.4.031057.

[6] P. W. Anderson, *An approximate quantum theory of the antiferromagnetic ground state*, Phys. Rev. **86**, 694 (1952), doi:10.1103/PhysRev.86.694.

[7] J. Hubbard, *Electron correlations in narrow energy bands*, Proceedings of the Royal Society of London. Series A. Mathematical and Physical Sciences **276**(1365), 238 (1963), doi:10.1098/rspa.1963.0204.

[8] N. F. Mott, *The basis of the electron theory of metals, with special reference to the transition metals*, Proceedings of the Physical Society. Section A **62**(7), 416 (1949), doi:10.1088/0370-1298/62/7/303.

[9] T. Maier, M. Jarrell, T. Pruschke and M. H. Hettler, *Quantum cluster theories*, Rev. Mod. Phys. **77**, 1027 (2005), doi:10.1103/RevModPhys.77.1027.

[10] G. Rohringer, H. Hafermann, A. Toschi, A. A. Katanin, A. E. Antipov, M. I. Katsnelson, A. I. Lichtenstein, A. N. Rubtsov and K. Held, *Diagrammatic routes to nonlocal correlations beyond dynamical mean field theory*, Rev. Mod. Phys. **90**, 025003 (2018), doi:10.1103/RevModPhys.90.025003.

[11] A. Georges, G. Kotliar, W. Krauth and M. J. Rozenberg, *Dynamical mean-field theory of strongly correlated fermion systems and the limit of infinite dimensions*, Rev. Mod. Phys. **68**, 13 (1996), doi:10.1103/RevModPhys.68.13.

[12] R. Rossi, *Determinant diagrammatic Monte Carlo algorithm in the thermodynamic limit*, Phys. Rev. Lett. **119**, 045701 (2017), doi:10.1103/PhysRevLett.119.045701.

[13] R. Garioud, F. Šimkovic IV, R. Rossi, G. Spada, T. Schäfer, F. Werner and M. Ferrero, *Symmetry-broken perturbation theory to large orders in antiferromagnetic phases* (2023), 2210.17423.

[14] A. Eberlein and W. Metzner, *Effective interactions and fluctuation effects in spin-singlet superfluids*, Phys. Rev. B **87**, 174523 (2013), doi:10.1103/PhysRevB.87.174523.

[15] E. A. Stepanov, S. Brener, F. Krien, M. Harland, A. I. Lichtenstein and M. I. Katsnelson, *Effective Heisenberg model and exchange interaction for strongly correlated systems*, Phys. Rev. Lett. **121**, 037204 (2018), doi:10.1103/PhysRevLett.121.037204.

[16] D. Geffroy, J. Kaufmann, A. Hariki, P. Gunacker, A. Hausoel and J. Kuneš, *Collective modes in excitonic magnets: Dynamical mean-field study*, Phys. Rev. Lett. **122**, 127601 (2019), doi:10.1103/PhysRevLett.122.127601.

[17] L. Del Re and A. Toschi, *Dynamical vertex approximation for many-electron systems with spontaneously broken SU(2) symmetry*, Phys. Rev. B **104**, 085120 (2021), doi:10.1103/PhysRevB.104.085120.

[18] X. Dong, L. D. Re, A. Toschi and E. Gull, *Mechanism of superconductivity in the hubbard model at intermediate interaction strength*, Proceedings of the National Academy of Sciences **119**(33), e2205048119 (2022), doi:10.1073/pnas.2205048119.

[19] K. Vasiliou, Y. He and N. Bultinck, *Electrons interacting with Goldstone modes and the rotating frame* (2023), `2307.05699`.

[20] I. A. Goremykin and A. A. Katanin, *Commensurate and spiral magnetic order in the doped two-dimensional Hubbard model: Dynamical mean-field theory analysis*, Phys. Rev. B **107**, 245104 (2023), doi:10.1103/PhysRevB.107.245104.

[21] Y. M. Vilk, L. Chen and A.-M. S. Tremblay, *Theory of spin and charge fluctuations in the Hubbard model*, Phys. Rev. B **49**, 13267 (1994), doi:10.1103/PhysRevB.49.13267.

[22] Y. M. Vilk and A.-M. S. Tremblay, *Non-perturbative many-body approach to the Hubbard model and single-particle pseudogap*, J. Phys. I France **7**(11), 1309 (1997), doi:10.1051/jp1:1997135.

[23] A.-M. Daré, Y. M. Vilk and A. M. S. Tremblay, *Crossover from two- to three-dimensional critical behavior for nearly antiferromagnetic itinerant electrons*, Phys. Rev. B **53**, 14236 (1996), doi:10.1103/PhysRevB.53.14236.

[24] A.-M. Daré and G. Albinet, *Magnetic properties of the three-dimensional Hubbard model at half filling*, Phys. Rev. B **61**, 4567 (2000), doi:10.1103/PhysRevB.61.4567.

[25] K. Zantout, S. Backes and R. Valentí, *Two-particle self-consistent method for the multi-orbital Hubbard model*, Annalen der Physik **533**(2), 2000399 (2021), doi:https://doi.org/10.1002/andp.202000399.

[26] K. Zantout, S. Backes and R. Valentí, *Effect of nonlocal correlations on the electronic structure of lifeas*, Phys. Rev. Lett. **123**, 256401 (2019), doi:10.1103/PhysRevLett.123.256401.

[27] O. Simard and P. Werner, *Nonequilibrium two-particle self-consistent approach*, Phys. Rev. B **106**, L241110 (2022), doi:10.1103/PhysRevB.106.L241110.

[28] C. Gauvin-Ndiaye, C. Lahaie, Y. M. Vilk and A. M. S. Tremblay, *An improved two-particle self-consistent approach* (2023), `2305.19219`.

[29] T. Moriya and A. Kawabata, *Effect of spin fluctuations on itinerant electron ferromagnetism*, Journal of the Physical Society of Japan **34**(3), 639 (1973), doi:10.1143/JPSJ.34.639, `https://doi.org/10.1143/JPSJ.34.639`.

[30] T. Moriya and A. Kawabata, *Effect of spin fluctuations on itinerant electron ferromagnetism. ii*, Journal of the Physical Society of Japan **35**(3), 669 (1973), doi:10.1143/JPSJ.35.669, `https://doi.org/10.1143/JPSJ.35.669`.

[31] A. A. Katanin, A. Toschi and K. Held, *Comparing pertinent effects of antiferromagnetic fluctuations in the two- and three-dimensional Hubbard model*, Phys. Rev. B **80**, 075104 (2009), doi:10.1103/PhysRevB.80.075104.

[32] G. Rohringer and A. Toschi, *Impact of nonlocal correlations over different energy scales: A dynamical vertex approximation study*, Phys. Rev. B **94**, 125144 (2016), doi:10.1103/PhysRevB.94.125144.

[33] J. Stobbe and G. Rohringer, *Consistency of potential energy in the dynamical vertex approximation*, Phys. Rev. B **106**, 205101 (2022), doi:10.1103/PhysRevB.106.205101.

[34] D. Lessnich, C. Gauvin-Ndiaye, R. Valentí and A. M. S. Tremblay, *Spin hall conductivity in the Kane-Mele-Hubbard model at finite temperature* (2023), 2307.15652.

[35] D. Sénéchal, A.-M. Tremblay and C. Bourbonnais, eds., *Theoretical Methods for Strongly Correlated Electrons*, Springer-Verlag New York Berlin Heidelberg, doi:10.1007/b97552 (2004).

[36] A. V. Chubukov and D. M. Frenkel, *Renormalized perturbation theory of magnetic instabilities in the two-dimensional Hubbard model at small doping*, Phys. Rev. B **46**, 11884 (1992), doi:10.1103/PhysRevB.46.11884.

[37] K. Kuboki and H. Yamase, *Static spin susceptibility in magnetically ordered states*, Phys. Rev. B **96**, 064411 (2017), doi:10.1103/PhysRevB.96.064411.

[38] S. Moukouri, S. Allen, F. Lemay, B. Kyung, D. Poulin, Y. M. Vilk and A.-M. S. Tremblay, *Many-body theory versus simulations for the pseudogap in the hubbard model*, Phys. Rev. B **61**, 7887 (2000), doi:10.1103/PhysRevB.61.7887.

[39] L. Del Re, M. Capone and A. Toschi, *Dynamical vertex approximation for the attractive hubbard model*, Phys. Rev. B **99**, 045137 (2019), doi:10.1103/PhysRevB.99.045137.

[40] T. Cea and L. Benfatto, *Nature and raman signatures of the higgs amplitude mode in the coexisting superconducting and charge-density-wave state*, Phys. Rev. B **90**, 224515 (2014), doi:10.1103/PhysRevB.90.224515.

[41] T. Cea, C. Castellani, G. Seibold and L. Benfatto, *Nonrelativistic dynamics of the amplitude (higgs) mode in superconductors*, Phys. Rev. Lett. **115**, 157002 (2015), doi:10.1103/PhysRevLett.115.157002.

[42] J. Lorenzana and G. Seibold, *Long-lived higgs modes in strongly correlated condensates*, Phys. Rev. Lett. **132**, 026501 (2024), doi:10.1103/PhysRevLett.132.026501.

[43] J. Koepsell, D. Bourgund, P. Sompet, S. Hirthe, A. Bohrdt, Y. Wang, F. Grusdt, E. Demler, G. Salomon, C. Gross and I. Bloch, *Microscopic evolution of doped mott insulators from polaronic metal to fermi liquid*, Science **374**(6563), 82 (2021), doi:10.1126/science.abe7165.

[44] G.-H. Huang and Z. Wu, *Magnetic correlations of a doped and frustrated Hubbard model: benchmarking the two-particle self-consistent theory against a quantum simulator* (2023), 2310.11263.

[45] A. Mazurenko, C. S. Chiu, G. Ji, M. F. Parsons, M. Kanász-Nagy, R. Schmidt, F. Grusdt, E. Demler, D. Greif and M. Greiner, *A cold-atom fermi–hubbard antiferromagnet*, Nature **545**(7655), 462 (2017), doi:10.1038/nature22362.

[46] L. Del Re and G. Rohringer, *Fluctuations analysis of spin susceptibility: Néel ordering revisited in dynamical mean field theory*, Phys. Rev. B **104**, 235128 (2021), doi:10.1103/PhysRevB.104.235128.

[47] V. Harkov, A. I. Lichtenstein and F. Krien, *Parametrizations of local vertex corrections from weak to strong coupling: Importance of the hedin three-leg vertex*, Phys. Rev. B **104**, 125141 (2021), doi:10.1103/PhysRevB.104.125141.